ELSEVIER

Comput. Methods Appl. Mech. Engrg. 190 (2000) 707–719

Computer methods in applied mechanics and engineering

www.elsevier.com/locate/cma

Branch switching techniques for bifurcation in soil deformation

Hilda van der Veen [a], Kees Vuik [b], René de Borst [c,*]

[a] *Faculty of Civil Engineering and Geosciences, Koiter Institute Delft, Delft University of Technology, P.O. Box 5048, 2600 GA Delft, The Netherlands*

[b] *Department of Applied Mathematics, Faculty of Information Technology and Systems, Delft University of Technology, P.O. Box 356, 2600 AJ Delft, The Netherlands*

[c] *Faculty of Aerospace Engineering, Koiter Institute Delft, Delft University of Technology, P.O. Box 5058, 2600 GB Delft, The Netherlands*

Received 25 June 1998

Abstract

The transition from homogeneous to localized deformations during the loading of a soil specimen within a finite element computation is often characterized by a bifurcation point, indicating loss of uniqueness of the solution. The signalling of a bifurcation point is done via the eigenvalues of the structural stiffness matrix resulting from the finite element discretization. Eigenvectors related to negative eigenvalues can be used to perturb a homogeneous state and to obtain a localized deformation mode. This procedure is called branch switching. Several methods are proposed to perform this branch switching. © 2000 Elsevier Science S.A. All rights reserved.

Keywords: Bifurcation; Localization; Branch-switching; Perturbation; Plasticity; Eigenvalues

1. Introduction

Soil is a difficult material to model, but of importance for e.g., the building of infrastructures and the oil industry. The homogeneous deformation of soil can be modeled quite well in contrast to the regime beyond homogeneous deformations, i.e., that of localized deformations. The transition from homogeneous to localized deformation is frequently characterized by a bifurcation point, indicating loss of uniqueness of the solution. A bifurcation point in the solution path is often (and typically so in the examples considered here) a consequence of spatial symmetry and of the homogeneous distribution of material parameters. At a certain load level, there may be more than one possible solution but most paths will be unstable. Material perturbation is a generally accepted method to circumvent the problem of loss of uniqueness [5]. This, however, may influence the peak load and the post-bifurcation deformation mode.

de Borst [1] has shown how the eigenvectors related to negative eigenvalues can be used to perturb a homogeneous state and to arrive at a path associated to localized deformation. This procedure is called branch switching. Here, it is shown how the method can be extended to account for more than one eigenvector associated to a negative eigenvalue. The orthogonality requirement of this perturbation may be too strict and not appropriate for the evolving localized deformation. For this reason an alternative method was developed, which is called deflation. It uses right and left eigenvectors of the tangent stiffness matrix to

* Corresponding author.
E-mail address: r.deborst@lr.tudelft.nl (R. de Borst).

0045-7825/00/$ - see front matter
PII: S0045-7825(99)00439-9

establish an incremental displacement vector which is related to a new tangent stiffness matrix with positive eigenvalues only.

The outline of the article is as follows. In Section 2 the most important characteristics of the soil model are described, including the yield function and the plastic flow law, the finite element model and the concept of bifurcation. In Section 3 the perturbation methods are discussed, first the orthogonal perturbation and then the deflation method. In Section 3.3 these two types of perturbation are related to each other. This is followed by a description of the perturbation methods, but with use of Schur vectors instead of eigenvectors, which leads to a considerable improvement of the efficiency. In Section 4 the results of a pure shear test and several biaxial compression tests (Section 4.2) are discussed.

2. Overview of the model

In this section we present a short overview of the most important characteristics of soil plasticity. The constitutive law, the yield surface and the kinematic relation are briefly discussed as well as the finite element discretization.

2.1. Material laws

A constitutive law describes the relation between stresses $\boldsymbol{\sigma}$ and strains $\boldsymbol{\epsilon}$. The elastic response is described by Hooke's law: $\boldsymbol{\sigma} = \mathbf{D}_e\boldsymbol{\epsilon}$, whereas the total elasto-plastic response is given by

$$\dot{\boldsymbol{\sigma}} = \mathbf{D}_{ep}\dot{\boldsymbol{\epsilon}}, \quad \mathbf{D}_{ep} = \mathbf{D}_e - \frac{\mathbf{D}_e\mathbf{m}\mathbf{n}^T\mathbf{D}_e}{H + \mathbf{n}^T\mathbf{D}_e\mathbf{m}}, \tag{1}$$

in which H is a hardening parameter. The two vectors $\mathbf{m}$ and $\mathbf{n}$ are the direction of plastic flow and the normal to the yield surface, respectively. The Drucker–Prager yield surface is used to separate the stresses that lead to an elastic response from those that result in plastic deformation. The Drucker–Prager yield function reads:

$$f = \sqrt{3J_2} + \frac{6\sin\phi}{3-\sin\phi}p - \frac{6c\cos\phi}{3-\sin\phi}, \tag{2}$$

with J_2 the second invariant of the deviatoric stresses and p the hydrostatic pressure [6]. The parameters c and ϕ are the cohesion and the friction angle, respectively. The normal to the yield surface $n_i = \partial f/\partial\sigma_i$ changes with a change in friction angle ϕ. The components of the direction of plastic flow are obtained from $m_i = \partial g/\partial\sigma_i$, with g as f but with ϕ replaced by the dilatancy angle ψ of the material. If $\phi = \psi$ the normal to the yield surface equals the direction of plastic flow. Normally, soil is described better with a non-associated flow rule, i.e., $\phi \neq \psi$.

2.2. Finite element discretization

The weak formulation of the equilibrium condition inside the body and on its surface can be written as [6]

$$-\int_{\Omega_e}\delta\boldsymbol{\epsilon}^T\boldsymbol{\sigma}\,dV + \int_{\partial\Omega_e}\delta\mathbf{u}^T\mathbf{t}\,dS = 0, \tag{3}$$

with $\boldsymbol{\sigma}$ the stress vector, $\boldsymbol{\epsilon}$ the strain vector and $\mathbf{t}$ the vector of surface tractions. The volume of an element is denoted by Ω_e and its boundary by $\partial\Omega_e$. The vector $\mathbf{u}$ contains the displacements. In the examples considered in this article body forces are not included.

For finite loading steps the constitutive law (Eq. (1)) is linearized as follows:

$$\boldsymbol{\sigma} = \tilde{\boldsymbol{\sigma}} + \mathbf{D}_{ep}\Delta\boldsymbol{\epsilon}, \tag{4}$$

where $\tilde{\boldsymbol{\sigma}}$ is fixed and $\Delta\boldsymbol{\epsilon}$ is a strain increment. The nodal degrees of freedom of element l of the finite element mesh are denoted by $\mathbf{u}^{l_n}$. The global displacement of element l is denoted by $\mathbf{u}^l$ and is computed with the interpolation matrix $\mathbf{N}_l$:

$$\mathbf{u}^l = \mathbf{N}_l \mathbf{u}^{l_n}. \tag{5}$$

The elements of matrix $\mathbf{N}_l$ are functions of nodal coordinates. The kinematic equation relating strain and displacement reads: $\boldsymbol{\epsilon}^{l_n} = \mathbf{L}^{\mathrm{T}}\mathbf{u}^{l_n}$. The differential operator $\mathbf{L}$ is made up of derivatives in space coordinates. It now follows that

$$\boldsymbol{\epsilon}^{l_n} = \mathbf{L}^{\mathrm{T}}\mathbf{N}_l\mathbf{u}^{l_n} = \mathbf{B}\mathbf{u}^{l_n} \quad \text{with } \mathbf{B} = \mathbf{L}^{\mathrm{T}}\mathbf{N}_l. \tag{6}$$

With Eq. (6) and the linearized constitutive equation (4), Eq. (3) becomes for element l:

$$\begin{aligned}\int_{\Omega_e} \delta\boldsymbol{\epsilon}^{l_n^{\mathrm{T}}}\boldsymbol{\sigma}\,\mathrm{d}V &= \int_{\Omega_e} \delta\boldsymbol{\epsilon}^{l_n^{\mathrm{T}}}(\tilde{\boldsymbol{\sigma}} + \mathbf{D}_{\mathrm{ep}}\Delta\boldsymbol{\epsilon}^{l_n})\,\mathrm{d}V \\ &= \int_{\Omega_e} \delta\mathbf{u}^{l_n^{\mathrm{T}}}\mathbf{B}^{\mathrm{T}}\mathbf{D}_{\mathrm{ep}}\mathbf{B}\Delta\mathbf{u}^{l_n}\,\mathrm{d}V + \int_{\Omega_e} \delta\mathbf{u}^{l_n^{\mathrm{T}}}\mathbf{B}^{\mathrm{T}}\tilde{\boldsymbol{\sigma}}\,\mathrm{d}V \\ &= \int_{\partial\Omega_e} (\mathbf{N}_l\delta\mathbf{u}^{l_n})^{\mathrm{T}}\mathbf{t}\,\mathrm{d}S. \end{aligned} \tag{7}$$

The nodal displacements do not depend on the space variables and can be taken out of the integral. Defining:

$$\mathbf{K}^l = \int_{\Omega_e} \mathbf{B}^{\mathrm{T}}\mathbf{D}_{\mathrm{ep}}\mathbf{B}\,\mathrm{d}V, \quad \Delta\mathbf{f}^l = \int_{\partial\Omega_e} \mathbf{N}_l^{\mathrm{T}}\mathbf{t}\,\mathrm{d}S - \int_{\Omega_e} \mathbf{B}^{\mathrm{T}}\tilde{\boldsymbol{\sigma}}\,\mathrm{d}V, \tag{8}$$

Eq. (7) becomes

$$\delta\mathbf{u}^{l_n^{\mathrm{T}}}\mathbf{K}^l\Delta\mathbf{u}^{l_n} = \delta\mathbf{u}^{l_n^{\mathrm{T}}}\Delta\mathbf{f}^l. \tag{9}$$

This relation holds for a specific element. The relation of all elements is thus expressed as:

$$\delta\mathbf{u}^{\mathrm{T}}\{\mathbf{K}\Delta\mathbf{u} - \Delta\mathbf{f}\} = 0. \tag{10}$$

In $\mathbf{K}$ and $\mathbf{f}$ all element contributions are assembled and $\mathbf{u}$ is the vector of all nodal displacements. The equation must hold for every virtually admissible nodal displacement vector $\delta\mathbf{u}$ and thus $\mathbf{K}\Delta\mathbf{u} = \Delta\mathbf{f}$ must hold.

The iterative Newton–Raphson [2] iteration is used to solve the incremental finite element equations. The total force is applied in small increments. Eq. (10) can therefore also be written as:

$$\mathbf{K}_i\Delta_i\mathbf{u} = \mu_i\mathbf{q}, \tag{11}$$

where Δ_i denotes the ith increment of the Newton–Raphson iteration. Vector $\mathbf{q}$ is fixed during the whole process, whereas parameter μ_i can be different for every increment.

2.3. Bifurcation

Bifurcation of the load–displacement path is defined as loss of uniqueness, which means that there exist more than one displacement increment that satisfies the incremental equilibrium (Eq. (11)). In here, the focus is on continuous bifurcations for which the same tangent stiffness matrix relates the possible displacement increments to the force increment. Suppose $\mathbf{K}_i\Delta_i\mathbf{u} = \mu_i\mathbf{q}$ has two solutions $\Delta_i\mathbf{u}$ for one μ_i. Subtracting the appropriate incremental relations and leaving out the subscripts, gives the bifurcation condition:

$$\mathbf{K}(\Delta^1\mathbf{u} - \Delta^2\mathbf{u}) = \mathbf{K}\Delta^{1-2}\mathbf{u} = 0 \tag{12}$$

with $\Delta^1\mathbf{u}$ and $\Delta^2\mathbf{u}$ the two possible displacement increments, and $\Delta^{1-2}\mathbf{u}$ their difference. Eq. (12) implies that $\mathbf{K}$ must be singular, i.e., at least one eigenvalue must equal zero. Let $\lambda_j, j = 1, \ldots, k$ be the zero eigenvalues

and $\mathbf{x}_j, \mathbf{y}_j$ the associated right and left eigenvectors. Because $\mathbf{K}$ is singular, a non-trivial solution of Eq. (12) exists if $\mu_i = 0$ or if $\mathbf{q}$ lies in the column space of $\mathbf{K}$ so that $\mathbf{y}_j^{\mathrm{T}}\mathbf{q} = 0$ for all j. The latter is called a bifurcation point. Note that for the examples discussed here, zero eigenvalues or an exact bifurcation point are never found. This is due to the fact that neither the material model nor the load increment procedure are continuous. Therefore, a change from loading to unloading results in a change of tangent stiffness matrix and a discontinuity in the load–displacement curve. In the examples of Section 3.2 it is assumed that a bifurcation point is passed if at least one eigenvalue is negative. For a symmetric matrix it holds that a negative eigenvalue exists if negative pivots arise, but for non-symmetric matrices only an odd number of negative pivots assures the presence of negative eigenvalues. However, it has been found that the signalling of negative eigenvalues via negative pivots is quite accurate [9].

3. Branch switch procedures

In this section several methods are discussed that can be used to obtain a localized deformation mode by perturbing the homogeneous solution with eigenvectors related to negative eigenvalues that arise if uniqueness is lost. For all methods it holds that after the perturbation, the solution vector is renormalized to its original length.

3.1. Orthogonal perturbation

The method described by de Borst [1] is set up with one eigenvector related to a negative eigenvalue and is recapitulated briefly. It is then extended so that it can handle more than one negative eigenvalue.

A bifurcation point is defined by a system matrix with at least one zero eigenvalue (Section 2) while the displacement is not stationary. If, at this point, a right eigenvector associated to a zero eigenvalue is added to the incremental displacement vector, another solution is obtained for the same problem, because

$$\mathbf{K}\{\Delta\mathbf{u} + \alpha\mathbf{x}\} = \mathbf{K}\Delta\mathbf{u}, \tag{13}$$

with $\mathbf{x}$ the right eigenvector related to the zero eigenvalue and α a non-zero weight factor. In practice, $\mathbf{x}$ is related to a (slightly) negative eigenvalue. This perturbation thus consists of adding the eigenvector $\mathbf{x}$ multiplied by α to the homogeneous solution

$$\tilde{\mathbf{u}} = \mathbf{u} + \alpha\mathbf{x}, \tag{14}$$

where α is chosen such that $\tilde{\mathbf{u}} \perp \mathbf{u}$. The parameter α is then given by

$$\alpha = -\frac{\mathbf{u}^{\mathrm{T}}\mathbf{u}}{\mathbf{x}^{\mathrm{T}}\mathbf{u}}. \tag{15}$$

For eigenvectors $\mathbf{x}$ that are almost orthogonal to the displacement vector $\mathbf{u}$, the weight factor α is very large. For more negative eigenvalues, the method can be extended by summation of all $\alpha_l\mathbf{x}_l$ for every eigenvector $\mathbf{x}_l$

$$\tilde{\mathbf{u}} = k\mathbf{u} - \sum_{l=1}^{k} \frac{\mathbf{u}^{\mathrm{T}}\mathbf{u}}{\mathbf{x}_l^{\mathrm{T}}\mathbf{u}}\mathbf{x}_l. \tag{16}$$

The number of negative eigenvalues k appears in the front of the right-hand side of the equation, in order to guarantee the orthogonality condition $\tilde{\mathbf{u}} \perp \mathbf{u}$ at the end of all eigenvector perturbations.

The method described in this section will be referred to as orthogonal perturbation and will be denoted by $\perp$.

3.1.1. Complex eigenvalues and eigenvectors

A non-symmetric matrix may possess complex eigenvalues. Although these were not found in the examples, they were encountered in previous studies [9]. A complex eigenvector can be incorporated in the perturbation without too much extra calculations and without introducing complexity in the solution.

Suppose that $\lambda = a + \mathrm{i}b$ is a complex eigenvalue with negative real part: $\mathrm{i}^2 = -1$ and $a < 0$. Since the tangent stiffness matrix is real, the complex conjugate of this eigenvalue $(a - \mathrm{i}b)$ is also present. The two associated pairs of right and left eigenvectors are denoted by $\mathbf{x}^{\mathrm{r}} + \mathrm{i}\mathbf{x}^{\mathrm{i}}, \mathbf{y}^{\mathrm{r}} + \mathrm{i}\mathbf{y}^{\mathrm{i}}$ and $\mathbf{x}^{\mathrm{r}} - \mathrm{i}\mathbf{x}^{\mathrm{i}}, \mathbf{y}^{\mathrm{r}} - \mathrm{i}\mathbf{y}^{\mathrm{i}}$. Suppose that only two eigenvalues are complex: $\lambda_1 = a + \mathrm{i}b$ and the associated complex conjugate $\lambda_2 = a - \mathrm{i}b$. The orthogonal perturbation (Eq. (16)) then reads:

$$\begin{aligned}\tilde{\mathbf{u}} &= 2\mathbf{u} - \frac{\mathbf{u}^{\mathrm{T}}\mathbf{u}}{(\mathbf{x}^{\mathrm{r}} + \mathrm{i}\mathbf{x}^{\mathrm{i}})^{\mathrm{T}}\mathbf{u}}(\mathbf{x}^{\mathrm{r}} + \mathrm{i}\mathbf{x}^{\mathrm{i}}) - \frac{\mathbf{u}^{\mathrm{T}}\mathbf{u}}{(\mathbf{x}^{\mathrm{r}} - \mathrm{i}\mathbf{x}^{\mathrm{i}})^{\mathrm{T}}\mathbf{u}}(\mathbf{x}^{\mathrm{r}} - \mathrm{i}\mathbf{x}^{\mathrm{i}}) \\ &= 2\mathbf{u} - \frac{\mathbf{u}^{\mathrm{T}}\mathbf{u}(\mathbf{x}^{\mathrm{r}} - \mathrm{i}\mathbf{x}^{\mathrm{i}})^{\mathrm{T}}\mathbf{u}(\mathbf{x}^{\mathrm{r}} + \mathrm{i}\mathbf{x}^{\mathrm{i}}) + \mathbf{u}^{\mathrm{T}}\mathbf{u}(\mathbf{x}^{\mathrm{r}} + \mathrm{i}\mathbf{x}^{\mathrm{i}})^{\mathrm{T}}\mathbf{u}(\mathbf{x}^{\mathrm{r}} - \mathrm{i}\mathbf{x}^{\mathrm{i}})}{(\mathbf{x}^{\mathrm{r}} + \mathrm{i}\mathbf{x}^{\mathrm{i}})^{\mathrm{T}}\mathbf{u}\,(\mathbf{x}^{\mathrm{r}} - \mathrm{i}\mathbf{x}^{\mathrm{i}})^{\mathrm{T}}\mathbf{u}} \\ &= 2\mathbf{u} - \frac{2\mathbf{u}^{\mathrm{T}}\mathbf{u}\,\mathbf{x}^{\mathrm{r}^{\mathrm{T}}}\mathbf{u}\,\mathbf{x}^{\mathrm{r}} + 2\mathbf{u}^{\mathrm{T}}\mathbf{u}\,\mathbf{x}^{\mathrm{i}^{\mathrm{T}}}\mathbf{u}\,\mathbf{x}^{\mathrm{i}}}{(\mathbf{x}^{\mathrm{r}^{\mathrm{T}}}\mathbf{u})^2 + (\mathbf{x}^{\mathrm{i}^{\mathrm{T}}}\mathbf{u})^2}.\end{aligned} \tag{17}$$

The cross products with imaginary terms cancel. More than one pair of complex eigenvalues can be processed in the same way.

3.2. Deflation

It is assumed that under displacement control (used consistently in this study) the emergence of negative eigenvalues in the systems matrix indicates a passage beyond a bifurcation point. Once the path has been found that relates to the critical localization mode, the system matrix will again have only positive eigenvalues. This property has been used in constructing a more general eigenvector perturbation method. All eigenvectors related to negative eigenvalues are considered, and the analysis is based on the right and left eigenvectors. In this manner the aspect of non-symmetry in case of non-associated plasticity problems is explicitly taken into account.

The basic idea was to perturb the matrix with negative eigenvalues just after bifurcation with the associated eigenvectors such that the negative eigenvalues are replaced by positive eigenvalues. This can be done by applying the deflation technique used often to obtain several eigenvalues from a matrix, see e.g., [7]. If $\lambda_l, l = 1, \ldots, k$ are the negative eigenvalues of $\mathbf{K}$, with associated right and left eigenvectors $\mathbf{x}_l, \mathbf{y}_l$, then the deflation of $\mathbf{K}$ can be written as follows:

$$\tilde{\mathbf{K}} = \mathbf{K} - \sum_{l=1}^{k} \omega_l \lambda_l \mathbf{x}_l \mathbf{y}_l^{\mathrm{T}}. \tag{18}$$

It is assumed that $\mathbf{x}_l$ is normalized to Euclidean length one and that $|\mathbf{y}_l^{\mathrm{T}}\mathbf{x}_l| = 1$. The deflation leaves all eigenvectors unchanged. This can be verified by post-multiplication by a right eigenvector. Also the positive eigenvalues are unperturbed. If $\omega_l = 1$ for all l then zero eigenvalues replace the negative eigenvalues. If $\omega_l > 1$ the negative eigenvalues turn positive with magnitude $(1 - \omega_l)\lambda_l$. Thus, all eigenvalues of $\tilde{\mathbf{K}}$ are again positive. For this reason ω_l is chosen larger than one.

Some first experiments were carried out, that perturbed the system matrix directly [11] with promising results. However, this method is computationally expensive. In general the system matrix is not assembled for the solution procedure, but all calculations are carried out on element level. However, to compute $\tilde{\mathbf{K}}$ assemblage of the element matrices is necessary. Moreover, the tangent stiffness matrix has a band structure that is destroyed by the perturbation. In [11] this was prevented by perturbing only the band, and hence introducing inaccuracies in the perturbation.

Due to the computational disadvantages of perturbing the system matrix directly, the method was further developed so that it would become more economic. Next, it is shown how the perturbation can be rewritten as a simple summation of vector updates.

In matrix form the deflation of (18) becomes

$$\tilde{\mathbf{K}} = \mathbf{K} - \mathbf{X}\mathbf{D}\mathbf{Y}^{\mathrm{T}}. \tag{19}$$

Here $\mathbf{D}$ is a diagonal matrix with entries equal to:

$$\begin{aligned} &d_l = \omega_l \lambda_l, \quad 1 \leqslant l \leqslant k, \\ &d_l = 0, \quad k < l \leqslant n. \end{aligned} \tag{20}$$

Note that Eq. (19) includes all eigenvectors but this is only necessary for the derivation of the simplified formulation. The final method makes use only of eigenvectors associated to negative eigenvalues.

A solution is sought of the equation $\tilde{\mathbf{K}}\Delta\tilde{\mathbf{u}} = \Delta\mathbf{f}$ (Eq. (10)). This equation relates increments of displacement to increments of force, where the solution is perturbed. In the following the Δs are left out of the equations for clarity. During this analysis it holds that $\tilde{\mathbf{u}} = \tilde{\mathbf{K}}^{-1}\mathbf{f}$. Of course, the inverse is never really computed in practice but a decomposition is made. The original and perturbed matrix can be decomposed into eigenvectors and eigenvalues as follows

$$\mathbf{K} = \mathbf{X}\mathbf{\Lambda}\mathbf{Y}^{\mathrm{T}}, \quad \tilde{\mathbf{K}} = \mathbf{X}\tilde{\mathbf{\Lambda}}\mathbf{Y}^{\mathrm{T}}, \quad \tilde{\mathbf{\Lambda}} = \mathbf{\Lambda} - \mathbf{D}. \tag{21}$$

For the derivation of the computationally more attractive deflation method the theoretical inverse in $\tilde{\mathbf{u}} = \tilde{\mathbf{K}}^{-1}\mathbf{f}$ is split into two parts. One part is the known $\mathbf{K}^{-1}$ of the unperturbed problem. The inverse of $\tilde{\mathbf{K}}$ can be written as

$$\tilde{\mathbf{K}}^{-1} = \mathbf{X}\tilde{\mathbf{\Lambda}}^{-1}\mathbf{Y}^{\mathrm{T}} = \mathbf{X}\mathbf{\Lambda}^{-1}\mathbf{Y}^{\mathrm{T}} - \mathbf{X}\tilde{\mathbf{D}}\mathbf{Y}^{\mathrm{T}} = \mathbf{K}^{-1} - \mathbf{X}\tilde{\mathbf{D}}\mathbf{Y}^{\mathrm{T}}. \tag{22}$$

The elements of $\tilde{\mathbf{D}}$ (not the inverse of $\mathbf{D}$ but part of the inverse of the non-singular $\tilde{\mathbf{\Lambda}}$), for $1 \leqslant l \leqslant k$, can be determined with Eq. (20) from

$$\frac{1}{\lambda_l - d_l} = \frac{1}{\lambda_l} - \tilde{d}_l \quad \Longleftrightarrow \quad \tilde{d}_l = \frac{-\omega_l}{\lambda_l(1-\omega_l)}. \tag{23}$$

For $k < l \leqslant n$ the elements $\tilde{d}_l$ are simply zero because $d_l = 0$. For the computation of $\tilde{\mathbf{u}}$, $\tilde{\mathbf{K}}^{-1}\mathbf{f}$ is split as follows:

$$\tilde{\mathbf{u}} = \tilde{\mathbf{K}}^{-1}\mathbf{f} = \mathbf{K}^{-1}\mathbf{f} - \mathbf{X}\tilde{\mathbf{D}}\mathbf{Y}^{\mathrm{T}}\mathbf{f} = \mathbf{u} - \mathbf{X}\tilde{\mathbf{D}}\mathbf{Y}^{\mathrm{T}}\mathbf{f}. \tag{24}$$

The last term can be written as a multiple vector update, leaving out the zero terms due to zero diagonal elements of $\tilde{\mathbf{D}}$

$$\tilde{\mathbf{u}} = \mathbf{u} - \sum_{l=1}^{k} \tilde{d}_l \mathbf{x}_l \mathbf{y}_l^{\mathrm{T}}\mathbf{f} = \mathbf{u} + \sum_{l=1}^{k} \frac{\omega_l \mathbf{y}_l^{\mathrm{T}}\mathbf{u}}{1-\omega_l}\mathbf{x}_l = \mathbf{u} + \sum_{l=1}^{k} \alpha_{\omega_l}\mathbf{x}_l \tag{25}$$

with $\alpha_{\omega_l} = \omega_l \mathbf{y}_l^{\mathrm{T}}\mathbf{u}/(1-\omega_l)$. In Eq. (25) the identity has been used that $\mathbf{y}_l^{\mathrm{T}}\mathbf{f} = \mathbf{y}_l^{\mathrm{T}}\mathbf{K}\mathbf{u} = \lambda_l \mathbf{y}_l^{\mathrm{T}}\mathbf{u}$. The perturbation has been simplified to several vector updates of the displacement vector with the eigenvectors related to negative eigenvalues.

The choice of ω_l is free as long as it is larger than one. If ω_l is taken constant, independent of the negative eigenvalue, a method arises denoted by ω_c. This method is referred to as constant deflation. If ω_l is different for each eigenvalue and such that the norm of the perturbation $\alpha_{\omega_l}\mathbf{x}_l$ for each $1 \leqslant l \leqslant k$ is equal to the norm of the unperturbed displacement vector a method evolves that is denoted by ω_n. The different ω_{n_l}s for this normalized deflation method are determined according to

$$\|\mathbf{u}\| = \left|\frac{\omega_{n_l}\mathbf{y}_l^{\mathrm{T}}\mathbf{u}}{1-\omega_{n_l}}\right| \|\mathbf{x}_l\| \quad \Longleftrightarrow \quad \omega_{n_l} = \frac{\|\mathbf{u}\|}{\|\mathbf{u}\| - |\,\mathbf{y}_l^{\mathrm{T}}\mathbf{u}\,|\,\|\mathbf{x}_l\|}, \tag{26}$$

where $\|\mathbf{x}_l\| = 1$ and $\omega_{n_l} > 1$. If $\|\mathbf{u}\|$ is less than $|\mathbf{y}_l^{\mathrm{T}}\mathbf{u}|$ the term on the right-hand side of Eq. (26) assigns a value less than one to ω_{n_l} which contradicts the assumption that $\omega_{n_l} > 1$. In practice this never happened. Note that $\alpha_{\omega_{n_l}}$ can be computed directly from the norm of $\mathbf{u}$ but then it would be impossible to verify $\omega_{n_l} > 1$. This method is referred to as normalized (ω_n) deflation.

3.2.1. Complex eigenvalues and eigenvectors

For the deflation perturbation it is also possible to take into account the complex eigenvalues if they would occur. Suppose again that only two eigenvalues have become complex: $\lambda_1 = a + ib$ and the associated complex conjugate $\lambda_2 = a - ib$. The deflation of the homogeneous solution vector can then be simplified as follows:

$$\begin{aligned}\tilde{\mathbf{u}} &= \mathbf{u} + \frac{\omega_1(\mathbf{y}^{\mathrm{r}} + i\mathbf{y}^{\mathrm{i}})^{\mathrm{T}}\mathbf{u}}{1-\omega_1}(\mathbf{x}^{\mathrm{r}} + i\mathbf{x}^{\mathrm{i}}) + \frac{\omega_2(\mathbf{y}^{\mathrm{r}} - i\mathbf{y}^{\mathrm{i}})^{\mathrm{T}}\mathbf{u}}{1-\omega_2}(\mathbf{x}^{\mathrm{r}} - i\mathbf{x}^{\mathrm{i}}) \\ &= \mathbf{u} + \left\{\frac{\omega_1}{1-\omega_1} + \frac{\omega_2}{1-\omega_2}\right\}\left(\mathbf{y}^{\mathrm{r}^{\mathrm{T}}}\mathbf{u}\right)\mathbf{x}^{\mathrm{r}} - \left\{\frac{\omega_1}{1-\omega_1} + \frac{\omega_2}{1-\omega_2}\right\}\left(\mathbf{y}^{\mathrm{i}^{\mathrm{T}}}\mathbf{u}\right)\mathbf{x}^{\mathrm{i}} \\ &\quad + \left\{\frac{i\omega_1}{1-\omega_1} - \frac{i\omega_2}{1-\omega_2}\right\}\left(\mathbf{y}^{\mathrm{r}^{\mathrm{T}}}\mathbf{u}\right)\mathbf{x}^{\mathrm{i}} + \left\{\frac{i\omega_1}{1-\omega_1} - \frac{i\omega_2}{1-\omega_2}\right\}\left(\mathbf{y}^{\mathrm{i}^{\mathrm{T}}}\mathbf{u}\right)\mathbf{x}^{\mathrm{r}}. \end{aligned} \tag{27}$$

The imaginary cross products disappear if $\omega_1 = \omega_2$. For the constant deflation this is so by definition. For the normalized deflation ω_i is determined by the norm of the eigenvectors (Eq. (26)) and is therefore the same for the first eigenvalue and for the second eigenvalue, which is the complex conjugate of the first. The deflation perturbation with complex eigenvectors thus becomes

$$\tilde{\mathbf{u}} = \mathbf{u} + \frac{2\omega\mathbf{y}^{\mathrm{r}^{\mathrm{T}}}\mathbf{u}}{1-\omega}\mathbf{x}^{\mathrm{r}} - \frac{2\omega\mathbf{y}^{\mathrm{i}^{\mathrm{T}}}\mathbf{u}}{1-\omega}\mathbf{x}^{\mathrm{i}}. \tag{28}$$

Extension of the complex eigenvector perturbation to more complex eigenvectors is straightforward.

3.3. Relation between orthogonal perturbation and deflation

The deflation method as well as the orthogonal perturbation can, for one negative eigenvalue, be written as $\tilde{\mathbf{u}} = \mathbf{u} + \alpha\mathbf{x}$. Each method determines α in a different manner:

$$\omega \quad \Rightarrow \quad \alpha_\omega = \frac{\omega\mathbf{y}^{\mathrm{T}}\mathbf{u}}{1-\omega}, \tag{29}$$

$$\perp \quad \Rightarrow \quad \alpha_\perp = \frac{-\mathbf{u}^{\mathrm{T}}\mathbf{u}}{\mathbf{u}^{\mathrm{T}}\mathbf{x}}. \tag{30}$$

Accordingly, α_ω and $\alpha_\perp$ are equal if:

$$\frac{\omega\mathbf{y}^{\mathrm{T}}\mathbf{u}}{1-\omega} = -\frac{\mathbf{u}^{\mathrm{T}}\mathbf{u}}{\mathbf{u}^{\mathrm{T}}\mathbf{x}} \quad \Longleftrightarrow \quad \omega = \frac{\mathbf{u}^{\mathrm{T}}\mathbf{u}}{\mathbf{u}^{\mathrm{T}}\mathbf{u} - (\mathbf{y}^{\mathrm{T}}\mathbf{u})(\mathbf{u}^{\mathrm{T}}\mathbf{x})}. \tag{31}$$

The ω can therefore be chosen such that the deflation and the orthogonal perturbation methods are equal. However, the condition that $\omega > 1$ will not be satisfied if $(\mathbf{y}^{\mathrm{T}}\mathbf{u})(\mathbf{u}^{\mathrm{T}}\mathbf{x}) > \mathbf{u}^{\mathrm{T}}\mathbf{u}$. This happened occasionally in the examples discussed in Section 4.

3.4. Schur vectors

It can be attractive to use Schur vectors instead of eigenvectors. With Schur vectors an orthogonal reduction of $\mathbf{K}$ can be obtained as follows:

$$\mathbf{KS} = \mathbf{SR}, \tag{32}$$

with $\mathbf{R}$ an upper triangular matrix, $\mathbf{S}^{\mathrm{T}}\mathbf{S} = \mathbf{I}$ and $\mathbf{I}$ the identity matrix. All matrices are of the same dimensions. The eigenvalues of $\mathbf{K}$ are found on the diagonal of $\mathbf{R}$. If $\mathbf{K}$ is normal ($\mathbf{K}\mathbf{K}^{\mathrm{T}} = \mathbf{K}^{\mathrm{T}}\mathbf{K}$) then $\mathbf{R}$ equals the diagonal matrix of eigenvalues and $\mathbf{S}$ is the eigenvector matrix. A partial Schur decomposition is a decomposition with a Schur matrix that has less columns than rows to an upper triangular matrix that is accordingly of smaller dimension than $\mathbf{K}$. Of course, the eigenvalues of this upper triangular matrix approximate the eigenvalues of $\mathbf{K}$ better if the decomposition is more complete.

Schur vectors are mutually orthogonal and the ordinary deflation used to obtain more than one eigenvalue is often more stable if performed with Schur vectors [3,7]. Alternative perturbations are formed by using Schur vectors instead of right eigenvectors in Eq. (16) and instead of right and left eigenvectors in Eq. (25). In practice there was no visual difference between the Schur vectors and the eigenvectors when both are plotted as deformation modes. No serious improvement is therefore expected from this approach. An important advantage of the Schur decomposition is that there is no difference between right and left vectors. Therefore, with Schur vectors only half as many vectors need to be computed for the deflation perturbation.

4. Examples

In this section two different problems are analyzed, with several discretizations. In each example the prescribed displacement is continued and refined up to one hundredth of the initial step size, until negative pivots appear. These pivots are computed within the Gaussian elimination process to solve each of the load displacement increments.

Once negative pivots are found, the eigenvalues and the right and left eigenvectors are computed with the BILAPO method [10](Bi-Lanczos [8] with Partial Orthogonalization) whereas the Schur vectors are computed with Arnoldi's method [4]. With the BILAPO method right and left eigenvectors are computed at the same time, whereas Arnoldi's method computes only one set at a time. The BILAPO method is cheaper than running Arnoldi's method twice for a fixed number of iterations, although in practice the BILAPO method approaches the cost of running Arnoldi's method twice [9].

4.1. Pure shear

The first example is primarily chosen as a test case for the proposed branch switch methods. In Fig. 1(a) the loading case as well as the discretization is shown. Linear elements have been used with nodes only at the corners. Note that the right and left-hand sides of this element are linked by dependence relations in order to behave identically with respect to the horizontal and the vertical displacement so as to simulate the one-dimensional underlying configuration. With 12 linear elements the total number of nodal degrees of freedom is 52, but only 23 are free. During homogeneous deformations the rod may shorten, but it is not allowed to bend.

Softening is applied to the cohesion c. During loading it holds that if the softening parameter goes from 0 to 10, the cohesion diminishes from 0.01 to 0.001. Young's modulus equals to 1.8625 N/mm^2 and Poisson's

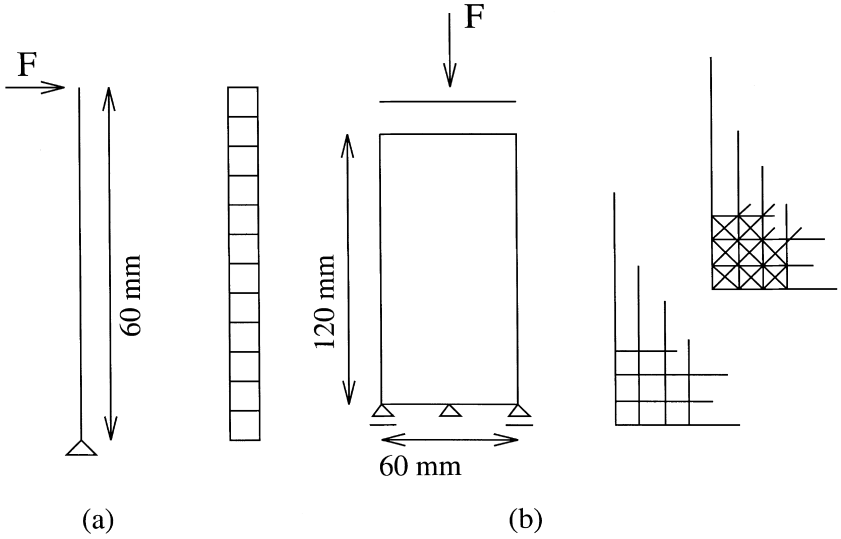

Fig. 1. Configuration and mesh of: (a) the pure shear test and (b) the biaxial compression test.

Table 1
Load [N] and displacement [mm] values, negative pivots and negative eigenvalues for bifurcation[a]

$\sin\psi$	Shear				Rectangles				Triangles		
	0.3	0.2	0.1	0.0	0.3	0.2	0.1	0.0	0.3	0.2	0.1
F	0.136	0.134	0.128	0.122	2.49	2.47	2.44	2.44	2.47	2.46	2.41
D	5.61	7.23	6.57	1.20	12.8	22.0	26.0	26.6	5.48	7.50	3.68
$p<0$	11	11	11	11	4	2	6	3	4	6	3
$\lambda<0$	11	11	11	11	4	2	4	1	4	6	1
$\perp$	−	−	−	−	+	+	−	−	+	+	−
ω_n	−	−	−	−	+	+	+	−	+	+	−
ω_c	+	+	+	+	+	+	+	−	−	+	−

[a] A plus sign indicates successful perturbation and a minus sign unsuccessful perturbation.

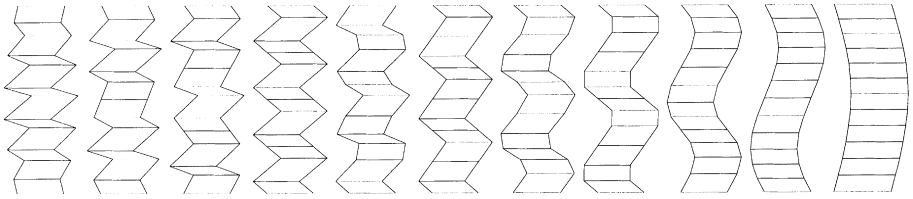

Fig. 2. Pure shear test. Eigenmodes associated to negative eigenvalues for $\sin\psi = 0.3$.

ratio $v = 0.49$. In the first block of Table 1 the load F and displacement D at which negative eigenvalues appear are summarized. These values are estimated in the top element. For all dilatancy angles that were investigated 11 negative eigenvalues and pivots were found. Only the constant deflation method worked well. The orthogonal perturbation and the normalized deflation methods caused localization in more than one element and negative pivots remained. For the zero dilatancy angle the bifurcation occurs at the onset of plastic deformation.

Fig. 2 shows all eigenmodes related to negative eigenvalues for $\sin\psi = 0.3$. The eigenmodes are similar for the other dilatancy angles.

4.2. Biaxial compression

The biaxial compression test consists of a two-dimensional specimen of 60×120 mm^2. The specimen is loaded at the top, supported at the bottom and the sides are free, see also Fig. 1(b). Softening is applied to the cohesion c, and Young's modulus equals 1.8625 N/mm^2. The friction angle is chosen such that $\sin\phi = 0.3$ whereas the dilatancy angle is varied: $\sin\psi = 0.3, 0.2, 0.1$. Two discretizations are considered, namely a mesh with rectangular quadratic elements and a mesh with triangular quadratic elements.

4.2.1. Rectangular mesh

A discretization of the biaxial compression test with 24×48 quadrilaterals with quadratic interpolation results in 7103 nodal degrees of freedom. For this test case the Poisson ratio is chosen equal to 0.3, and the softening is such that the cohesion decreases from 0.01 to 0.001 when the hardening parameter increases from 0 to 1000. The bifurcation load and displacement, the number of negative pivots and the number of negative eigenvalues is different for each of the dilatancy angles. The data are summarized in the second block of Table 1. This table also shows the results of the three variants of the eigenvector perturbation.

When the difference between the friction angle ϕ and the dilatancy angle ψ is small, all methods behave in a rather similar fashion. However, when this difference becomes large ($\sin\psi = 0.1$), differences arise. The normalized deflation shows no problems if $\sin\psi = 0.1$. With the constant deflation method negative pivots

remain, but gradually disappear in the increments after the perturbation. The final deformation is that of a reflected shearband. With the orthogonal perturbation the incremental deformation just after perturbation is that of a single shear band, but with significant extra localization in the rest of the specimen. This leads to the growth of multiple shearbands in later iterations and to a divergence of the Newton–Raphson iteration.

For a zero dilatancy angle none of the perturbation methods was successful. Two negative pivots appear before negative eigenvalues are found. When the number of negative pivots has reduced to one, a negative eigenvalue is also found. The associated eigenvector is strongly undulating. Perturbation with the orthogonal method or normalized deflation, leads to an unstable deformation similar to the eigenmode. With the constant deflation method the deformation remains homogeneous.

Fig. 3 shows some typical eigenmodes related to negative eigenvalues, and Fig. 4 some of the localized deformation modes.

4.2.2. Triangular mesh

The specimen deformed under biaxial loading is now discretized with 12×24 rectangles each of which is subdivided into four triangles, so that a problem with 4703 degrees of freedom arises. Poisson's ratio equals to 0.49 and the cohesion decreases from 0.01 to 0.001 when the hardening parameter increases from 0 to 10. The load and displacement values associated to the occurrence of negative pivots and eigenvalues are summarized in the last block of Table 1. In this table the performance of the perturbation methods is also represented. Constant deflation for $\sin\psi = 0.3$ resulted in a double shearband. For $\sin\psi = 0.1$ two negative pivots appeared before negative eigenvalues were found. Once the number of negative pivots had increased to three, a negative eigenvalue was found.

With a zero dilatancy angle the problem became uncontrollable. At the onset of plasticity 95 negative pivots appeared and this was considered unrealistic and the calculations were not continued.

Fig. 5 shows some typical eigenmodes related to negative eigenvalues, and Fig. 6 shows some of the localized deformation modes.

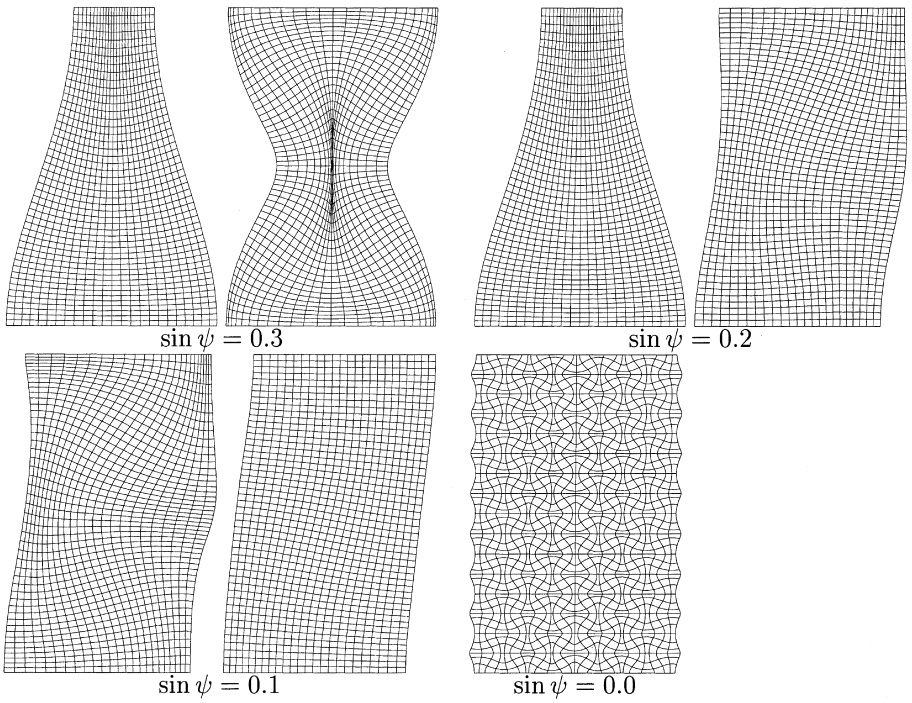

Fig. 3. Biaxial compression with rectangular elements. Eigenmodes associated to negative eigenvalues, farthest and closest to zero for different dilatancy angles.

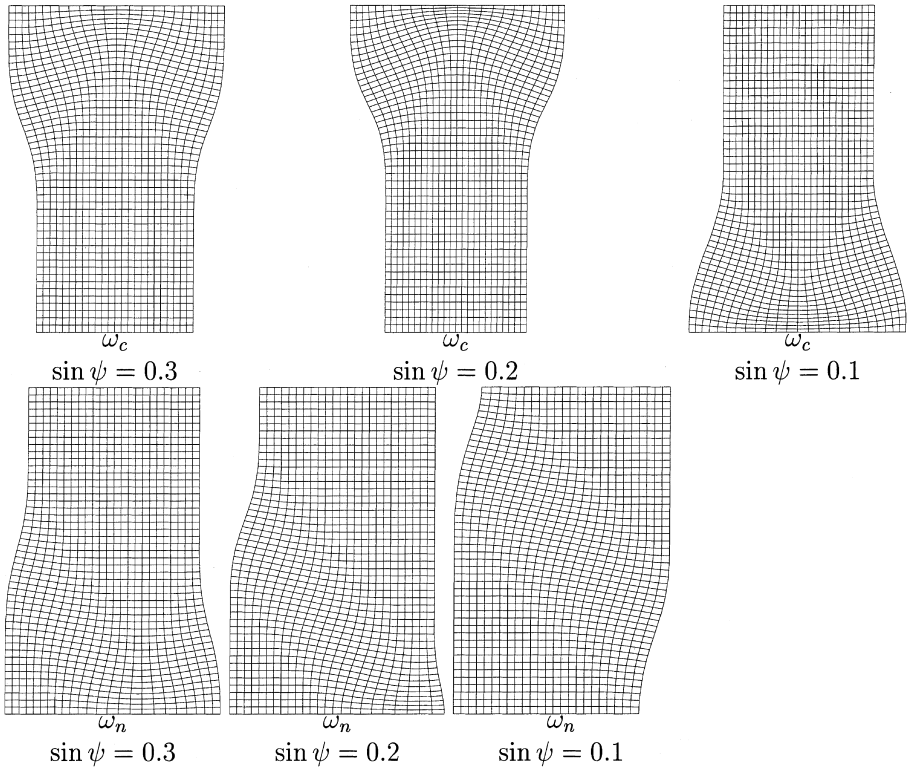

Fig. 4. Biaxial compression test with rectangular elements. Deformation modes found with constant deflation and with normalized deflation.

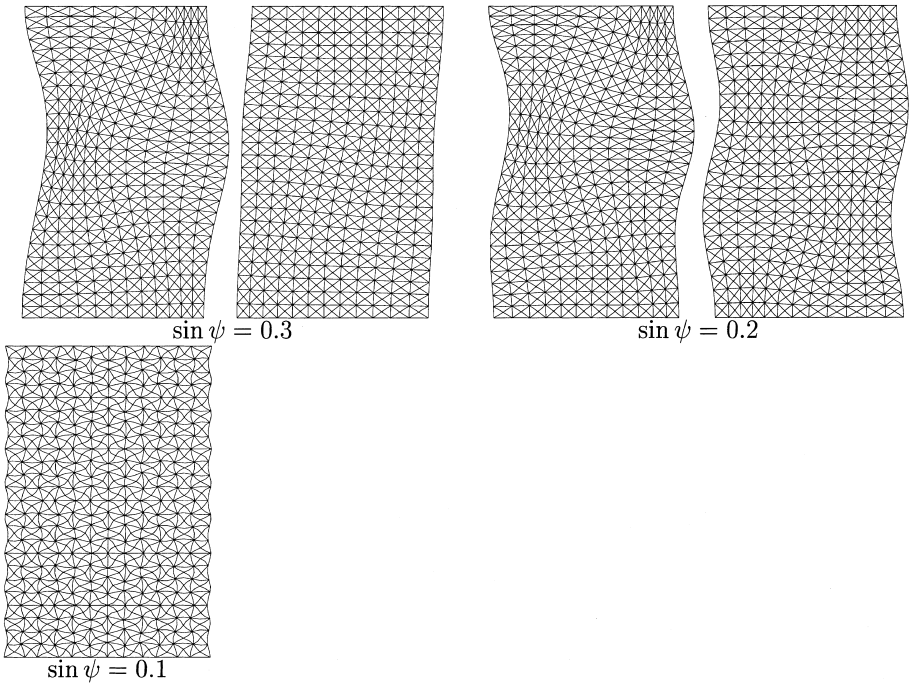

Fig. 5. Biaxial compression test with triangular elements. Eigenmodes associated to negative eigenvalues, farthest and closest to zero for different dilatancy angles.

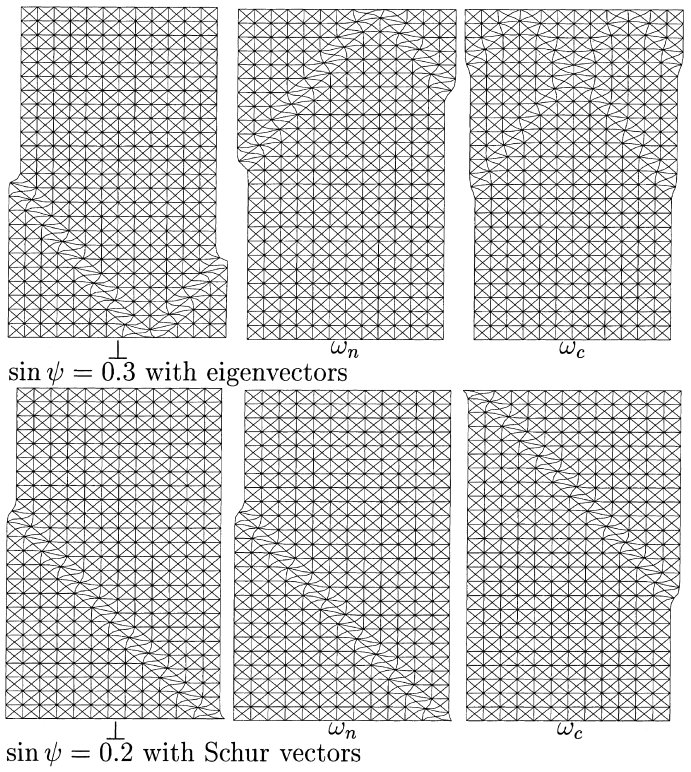

Fig. 6. Biaxial compression test with triangular elements. Deformation found with orthogonal perturbation, normalized deflation and constant deflation. The second three modes are obtained by perturbation with Schur vectors.

5. Conclusions

The orthogonal perturbation method [1] was generalized to include all eigenvectors associated to negative eigenvalues. This method worked satisfactorily, but the orthogonality requirement may be too strong. Therefore a new perturbation technique was developed that is more general. It is based on the idea that under displacement control a tangent stiffness matrix associated with a properly localized solution possesses no negative eigenvalues. This eigenvector perturbation method is called deflation and performs as well as the orthogonal perturbation.

Instead of eigenvectors it is possible to use Schur vectors. In the problems that have been investigated the performance was unchanged by substitution of Schur vectors at the place of eigenvectors in the perturbation. However, only half as many vectors need to be computed for the deflation perturbation if Schur vectors are used instead of eigenvectors. Moreover, the Schur vectors form an orthogonal set of vectors in contrast to eigenvectors of nonsymmetric matrices. This may improve the performance.

It is noteworthy that the signalling of bifurcation by negative pivots of the nonsymmetric tangent stiffness matrix **K** was quite accurate. In a few examples, where nonsymmetry was very pronounced, one or two negative pivots appeared prior to negative eigenvalues. An increase or a decrease of negative pivots to an odd number signalled the presence of negative eigenvalues and indicated a passage beyond a bifurcation point. The solution could then be steered onto a path associated to a localized deformation pattern with help of eigenvectors associated to negative eigenvalues.

Acknowledgements

The computations were performed in a pilot version of the finite element package DIANA that is maintained and developed at TNO Building and Construction Research, Rijswijk, The Netherlands.

References

[1] R. de Borst, Computation of post-bifurcation and post-failure behavior of strain- softening solids, Computers and Structures 25 (1987) 211–224.
[2] M.A. Crisfield, Non-linear Finite Element Analysis of Solids and Structures, vol. I, Wiley, West Sussex, UK, 1991.
[3] D.R. Fokkema, G.L.G. Sleijpen, H.A. van der Vorst, Jacobi–Davidson style QR and QZ algorithms for the partial reduction of matrix pencils, Preprint 941, University of Utrecht, The Netherlands, 1996.
[4] G.H. Golub, C.F. van Loan, Matrix Computations, third ed., The Johns Hopkins University Press, London, 1996.
[5] A.E. Groen, Three-dimensional elasto-plastic analysis of soils, Ph.D. thesis, Delft university of Technology, April 1997.
[6] J. Lubliner, Plasticity Theory, Macmillan, New York, 1990.
[7] Y. Saad, Numerical solution of large nonsymmetric eigenvalue problems, Computer Physics Communications 53 (166) (1989) 71–90.
[8] Y. Saad, Numerical Methods for Large Eigenvalue Problems, Manchester University Press, Manchester, 1992.
[9] H. van der Veen, The significance and use of eigenvalues and eigenvectors in the numerical analyusis of elasto-plastic soils, Ph.D. thesis, Delft University of Technology, 1998.
[10] H. van der Veen, C. Vuik, Bi-Lanczos with partial orthogonalization, Computers and Structures 56 (4) (1995) 605–613.
[11] H. van der Veen, C. Vuik, R. de Borst. Post-bifurcation behavior in soil plasticity: eigenvector perturvation compared to deflation, in: D.R.J. Owen, E. Oñate, E. Hinton (Eds.), Computational Plasticity; Fundamentals and Applications, Proceedings of the Fifth International Conference on Computational Plasticity, CIMNE, 1997, pp. 1745–1751.